

## SHORT COMMUNICATION

# In vivo contrast-enhanced microCT for the monitoring of mouse thoracic, lumbar, and coccygeal intervertebral discs

Remy E. Walk<sup>1</sup> | Simon Y. Tang<sup>1,2,3</sup> 

<sup>1</sup>Department of Biomedical Engineering, Washington University in St. Louis, St. Louis, Missouri

<sup>2</sup>Department of Mechanical Engineering and Materials Science, Washington University in St. Louis, St. Louis, Missouri

<sup>3</sup>Department of Orthopaedic Surgery, Washington University in St. Louis, St. Louis, Missouri

### Correspondence

Simon Y. Tang, Department of Orthopaedic Surgery, Washington University in St. Louis, 660 South Euclid Ave, Box 8233, St. Louis, MO 63110.

Email: simon.tang@wustl.edu

### Funding information

National Institutes of Health, Grant/Award Numbers: R01 AR074441, R21 AR069804, K01 AR069116, P30 AR 057235, T32 DK108742, UL1 TR002345; Washington University Musculoskeletal Research Center

### Abstract

Mouse models are often used for studies of intervertebral disc (IVD) homeostasis and degeneration, yet the relatively small size of the IVD poses challenges for noninvasive, longitudinal imaging modalities. The recently developed contrast-enhanced microCT (CE $\mu$ CT) using Ioversol has been successful in detecting degenerative changes in the murine IVD *ex vivo* at the micrometer scale. Further leveraging the superior biocompatibility of Ioversol as a contrast agent, we demonstrate the *in vivo* use of this CE $\mu$ CT technique to examine IVDs at multiple spinal sites. Ioversol was administered via tail vein injection (TVI) in growing and adult male FVB/NJ mice ( $n = 5$  /group). The animals were anesthetized and underwent *in vivo* micro-computed tomographic (microCT) at the coccygeal (CC5/CC6), lumbar (L5/6), and thoracic (T12/T13) IVDs. TVI of Ioversol was well-tolerated by all animals. As Ioversol filtered through the kidneys and accumulated in the bladder, the attenuations of the mouse bladder and kidneys increased due to the high molecular weight of Ioversol, confirming that the Ioversol is biologically available. Average IVD attenuations increased 3%-15% following TVI (ANOVA;  $P < .01$ ). The presence of Ioversol in the IVD combined with high-resolution microCT allow for nondestructive visualization of structural features of the IVD. These results demonstrate CE $\mu$ CT with Ioversol as a viable strategy for the *in vivo* monitoring of multiple mouse IVDs during degeneration, disease, and injury.

### KEYWORDS

aging, Contrast-enhanced microCT, intervertebral disc, mouse model

## 1 | INTRODUCTION

Low back pain is one of the most common causes of disability.<sup>1</sup> With intervertebral disc (IVD) degeneration being a leading contributor to the development of low back pain, there is a need for a better understanding of the biological and structural changes of the IVD that occur with the disease and injury.<sup>2</sup> Mouse models are useful for studying the molecular mechanisms of IVD biology because of the number of genetically modified models and established techniques to induce

degeneration.<sup>3</sup> However, resolving the micrometer-scale structural features of the mouse IVD remains a significant challenge even with state-of-the-art small animal microMRI technologies.<sup>4</sup>

Micro-computed tomographic (microCT) techniques have outstanding spatial resolution for the volumetric imaging of mineralized tissues in rodents.<sup>5</sup> However, since nonmineralized tissues do not attenuate X-Rays, a contrast agent is required to differentiate the soft tissue of interest. Although ionic and heavy-metal and ionic contrast-agents have shown to improve the X-ray attenuation of IVDs for

This is an open access article under the terms of the Creative Commons Attribution License, which permits use, distribution and reproduction in any medium, provided the original work is properly cited.

© 2019 The Authors. JOR Spine published by Wiley Periodicals, Inc. on behalf of Orthopaedic Research Society

ex vivo imaging<sup>6,7</sup>, the nonionic, hydrophilic, and highly biocompatible nature of Ioversol make it particularly suited for in vivo use.<sup>8</sup> Ioversol has been used clinically as a diagnostic radiographic contrast agent. With a high molecular weight, 807.115 g/mol, Ioversol reduces the x-rays that can pass through the tissue and increases the attenuation of blood vessels, organs, and other nonmineralized tissues. We have previously reported on a contrast-enhanced microCT (CE $\mu$ CT) technique using Ioversol to monitor and quantify IVD degeneration in vitro and ex vivo.<sup>9,10</sup> Extending this work further, the objective of this study is to explore and validate the in vivo use of CE $\mu$ CT technique using Ioversol to examine intervertebral discs at multiple spinal sites using growing and adult FVB/NJ mice.

## 2 | METHODS

### 2.1 | Animals

All procedures were performed with the approval of Washington University School of Medicine Institutional Animal Care and Use Committee. Male FVB/NJ mice at two age groups, 3- (growing) and 8- (adult) month old, were used in this study (n = 5 / group). Wild-type mice

were selected for this study to examine the diffusion of Ioversol into the IVD under healthy conditions. Mice were kept in standard husbandry conditions with 12-hour light/dark cycles as described by Jackson Labs (<https://www.jax.org/jax-mice-and-services/customer-support/technical-support/breeding-and-husbandry-support/mouse-room-conditions>). Mice were injected with 8 mL/kg of 350 mg/mL of Ioversol (OptiRay 350; Guerbet, St. Louis, Missouri) which reflects veterinary recommendations for a mouse at the highest available concentration of Ioversol. Mice were placed in a restrainer on a heat pad and lidocaine was applied to the tail. A 29G syringe was used to inject Ioversol into the lateral tail vein of the mouse. Mice were then anesthetized by isoflurane prior to microCT imaging.

### 2.2 | MicroCT imaging

MicroCT imaging was conducted on a VivaCT40 system (Scanco Medical, CH) at 10  $\mu$ m voxel size (45 kVp, 177  $\mu$ A, 116 ms integration time). Our preliminary studies showed that at least 20 minutes is required for TVI-administration of Ioversol to diffuse into the intradiscal space to increase the attenuation of the tissue. We

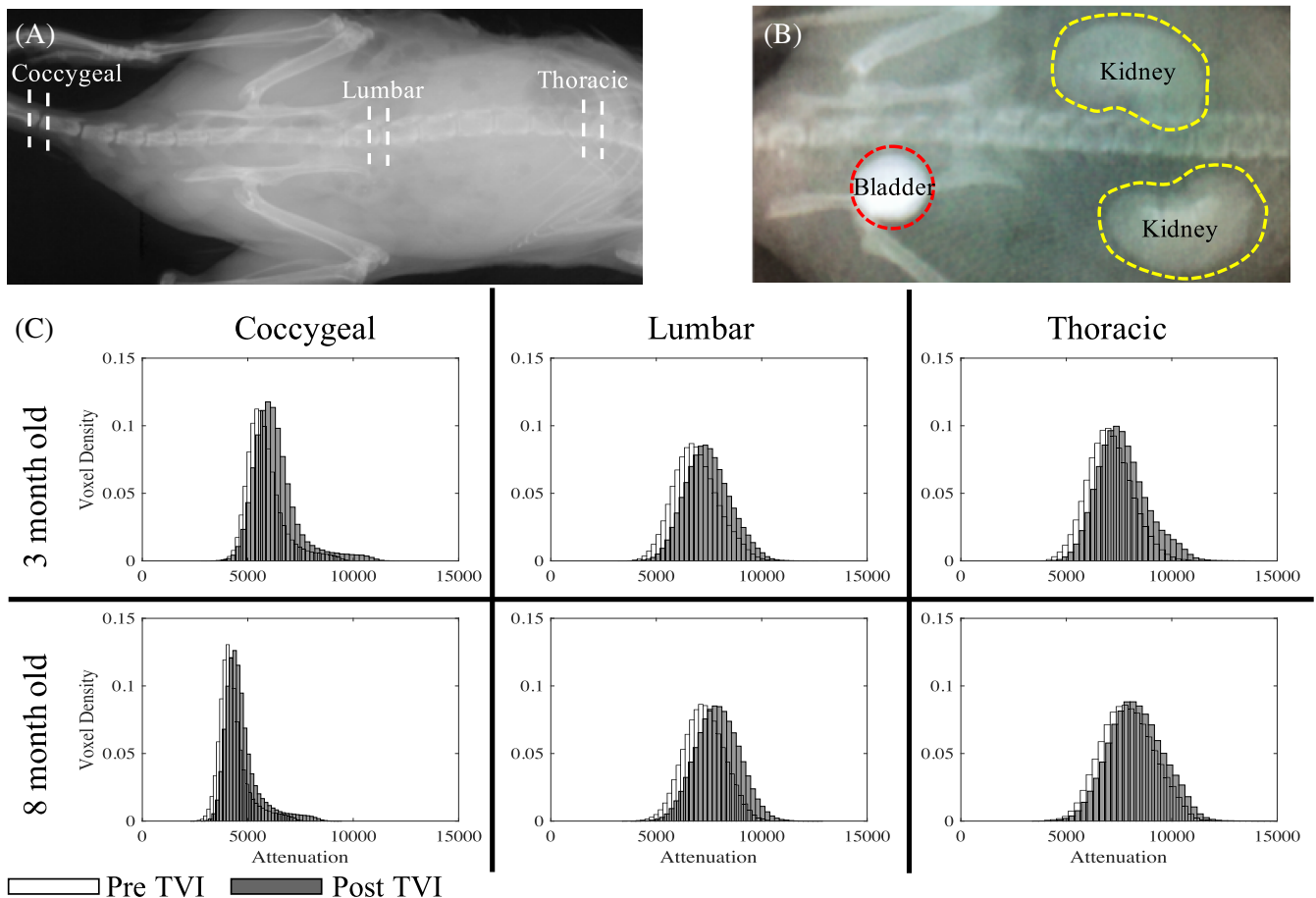


**FIGURE 1** A, A radiograph of mouse indicating the CC5/CC6, L5/L6, and T12/T13 IVDs that were scanned for this study. B, Bioavailability of Ioversol is confirmed by the increased attenuation of the bladder and kidneys approximately 15 minutes post-TVI. C, Typical histograms of pre-TVI and post-TVI scans of the three spinal levels in 3- and 8-month old mice. Injection with Ioversol shifts the histogram to the right and reduces the number of low attenuating voxels

observed that the bioavailability of loversol diminish significantly 2-hours post-TVI.

To determine the optimum time to achieve the maximum attenuation, each site is scanned at several timepoints following the injection. During the 110 minutes scanning period, three intervertebral levels (coccygeal [CC], lumbar [L], and thoracic [T]; Figure 1A) were scanned at three timepoints to observe the diffusion of loversol through different levels of the spinal column. The CC5/CC6, L5/L6, and T12/T13 IVDs were imaged for this study. CC5/CC6 was imaged at 20, 50, and 80 minutes; L5/L6 at 30, 60, and 90 minutes; and T12/T13 at 40, 70, and 100 minutes after injection. A scan at each site took approximately 8 minutes. The staggered timepoints at different sites were necessary to account for the times required for source and detector repositioning. A scan of each level was taken prior to injection with loversol to determine a baseline attenuation. The maximum attenuations from the three time points are determined and tabulated.

### 2.3 | Image processing

The raw data was exported to DICOM for further analysis using a custom MATLAB program (<https://github.com/WashUMRC/ContouringGUI>). Following an initial median filter (weight = 0.8, radius = 7), vertebral bodies were used as landmarks to remove the surrounding soft tissue. Contours were drawn around the outer edge of the vertebral bodies and morphed using linear interpolation. The bone was excluded to generate a mask of the IVD. The threshold was verified by visual inspection to ensure that all voxels containing bone were removed from the mask. The mask undergoes a morphological open followed by a morphological close to smooth edges and fill voids. From the mask of the whole disc, volume and average attenuation were calculated. The volume was determined from the total number of voxels included in the mask. The mean attenuation was taken as the average 16-bit grayscale value of the voxels contained within the mask. The mean attenuation of scans following TVI of loversol was normalized to their respective baseline scans. The ratio of the

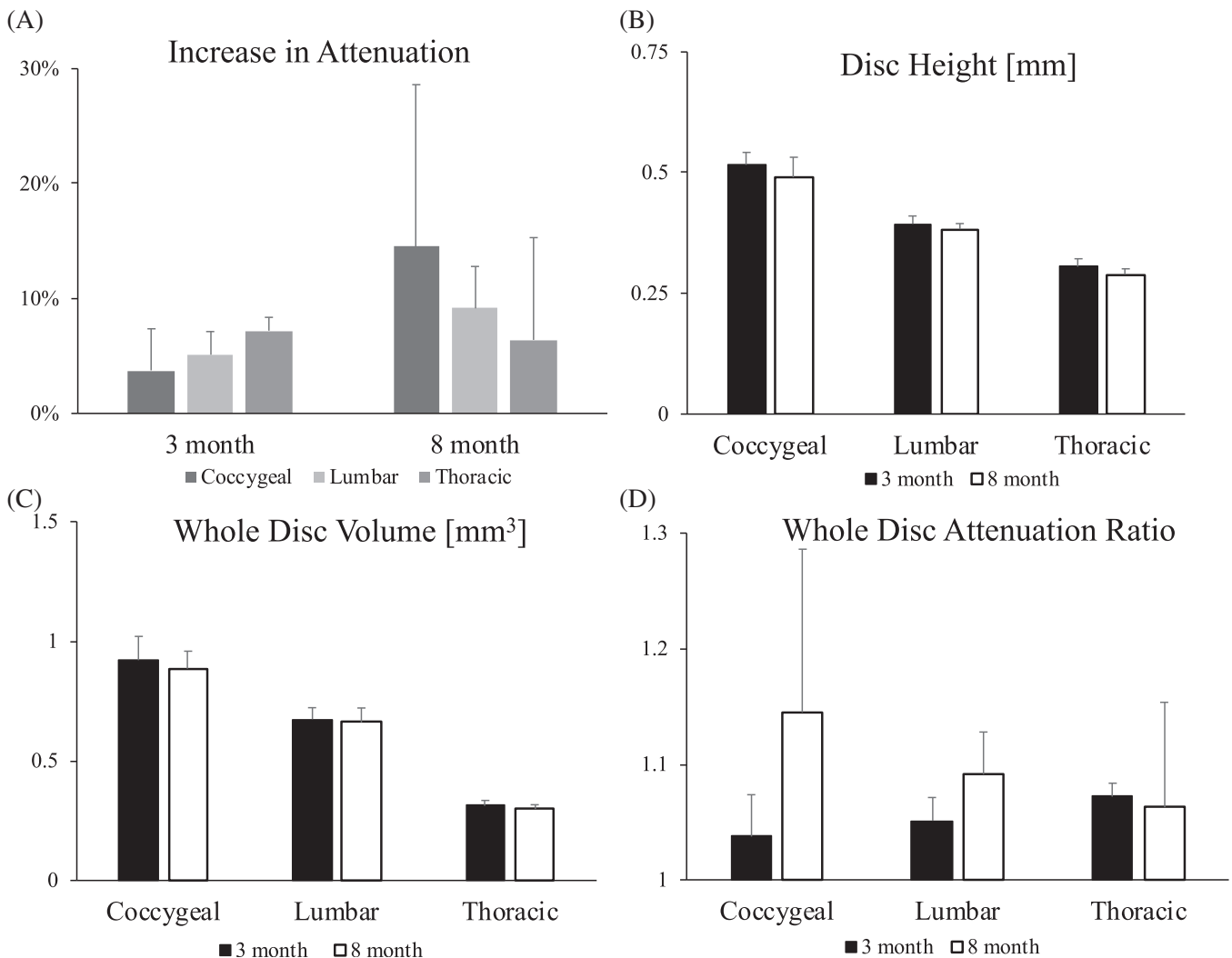


**FIGURE 2** A, TVI significantly increased the attenuations of the IVDs in the 3- and 8-month animals (3-way ANOVA;  $P < .01$ ). B and C, The 3D data enables the unbiased quantification of disc height and whole disc volume. D, The whole disc attenuation ratio ( $D1/D1_0$ ) increased in the adult lumbar IVDs

mean attenuation of the post-TVI scan ( $D_I$ ) to the pre-TVI ( $D_{I_0}$ ) was calculated for both groups at all levels. Disc heights and visualizations were obtained using OsiriX (Pixmeo, Geneva, Switzerland). Disc height represents the average disc height across five evenly spaced points along the mid-sagittal plane of the IVD.

## 2.4 | Statistics

A 3-way ANOVA was performed to determine the effect of age, spinal level, and loversol-injection on the attenuations of the IVDs. Statistical were conducted using RStudio 1.1.453 (RStudio, Boston, Massachusetts).

## 3 | RESULTS

Tail vein injection (TVI) of loversol was well-tolerated by the mice with no adverse events observed up to 4 weeks post injection. Shortly following TVI, the bladder and kidney became attenuating features in the microCT-scout view, confirming the metabolism and bioavailability of loversol (Figure 1B).

The post-TVI scans showed increased attenuations of the IVD regions compared with the pre-TVI scans. Qualitative inspection also showed that the IVD attenuation increased compared to other soft tissues in the IVD's vicinity. Quantitative comparisons of the voxel densities versus attenuations showed that the entire intradiscal region

shifts towards elevated values (Figure 1C), with the average increase ranging from 3% to 15% ( $P < .01$ ; Figure 2A,D). Moreover, there is a reduction in the number of low attenuating voxels. Taken together, the loversol delivered by TVI was biologically available, and the loversol was transported to the IVD where it was preferentially taken up compared to the surrounding soft tissues.

In order to explore the time-dependence of loversol retention in the IVD, we monitored each intervertebral disc at three timepoints as technically allowed by the microCT system. Mean attenuation varied by less than 5% between the three post-TVI scans (data not shown). Increased attenuation following injection with loversol was observed across all levels and ages (Figure 2A, D). At the coccygeal level, in both 3- and 8-month old mice, maximum attenuation was achieved 50 minutes after injection with loversol and maintained throughout the scanning period of the tail disc (50-90 minutes). The L5/L6 disc reached maximum attenuation at 30 minutes post-TVI in 3-month old mice and in 8-month old mice. At the thoracic level, a maximum attenuation achieved 40 minutes after TVI in both 3- and 8-month old mice that is maintained throughout the scanning of the T12/T13 IVD (40-110 minutes). Morphological parameters such as disc height and volume can be directly quantified from the microCT images (Figure 2B, C). No significant differences between ages were observed. Following contouring and segmentation, three-dimensional visualizations of the IVDs were rendered (Figure 3).

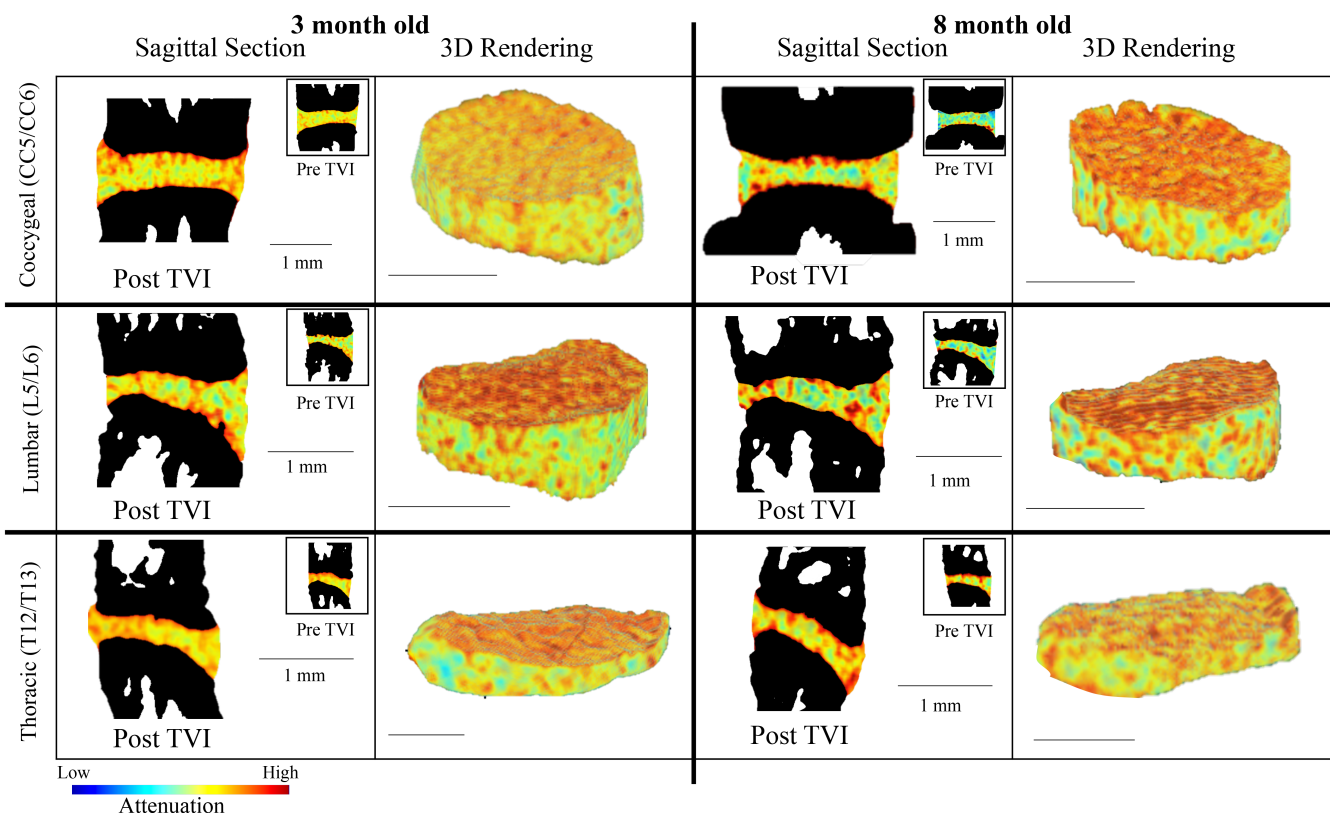


**FIGURE 3** 2D and 3D renderings of pre- and post-TVI of the CC5/CC6, L5/L6, and T12/T13 IVDs in 3- and 8-month old mice. The increased attenuations after TVI allowed for contouring of the IVD tissue boundary for the accurate 3D reconstructions of the IVD

## 4 | DISCUSSION

To date, this is the first study to describe the *in vivo* use of CE $\mu$ CT for the imaging of the mouse intervertebral disc. This approach was previously demonstrated in several *ex vivo* rodent models of IVD degeneration, and it achieved superior spatial resolution compared with microMRI.<sup>9,10</sup> By delivering loversol through tail-vein injection at a physiologically compatible dose, loversol was biologically available and accumulated preferentially in the IVD to increase the attenuation of all the scanned IVDs. We obtained disc height and volume measures of the IVDs expected from the aging mouse IVD.<sup>6,11,12</sup>

The TVIs were well-tolerated by all mice with no adverse consequences, suggesting that the technique would be suitable for longitudinal monitoring. However, it is worth noting that loversol is metabolized through the mouse quickly, and we observe declines in IVD and kidney signal as early as 120 minutes post-TVI. As the natural course of urinary homeostasis, the bladder attenuation increases over time until the loversol is expelled. This accumulation of contrast-agent in the bladder could occasionally introduce beam-hardening artifacts if the IVD of interest is localized near the bladder, and we would suggest users of this approach to be cognizant of the anatomical variations and metabolic rate of the mouse model. We observed that time required to achieve maximum attenuation depended on age of the animal and spinal level, and it may be important to optimize injection and imaging parameters for animals of different sex, strain, and backgrounds. Here, we were limited by the scan time and time for detector repositioning for optimizing post-TVI scan time; future work focused on a single level would allow additional timepoints to be investigated for further refinement of the optimal time between injection and post-TVI scan. The attenuation signals are influenced by motion and partial volume effects, and this is particularly evident in the thoracic IVD due to the narrow intradiscal space (approximately 100-200  $\mu$ m disc height) and proximity to the lungs during breathing. Motion artifacts and partial volume effects may have contributed to the variation in the attenuation response post-TVI. As a result, thoracic IVDs may not be suited for this technique. Yet the lumbar and coccygeal vertebrae did not exhibit motion artifacts, suggesting that motion was not a factor at these sites. It is worth noting that alterations in endplate porosity and hydration levels may also influence the infiltration of loversol and attenuation of the IVD following TVI. Our approach here accounts for these variations by scanning each spinal site at multiple timepoints to determine the time between injection and imaging to maximize the diffusion of loversol into the IVD. If only one or two adjacent IVDs were monitored, the signal-to-noise can be improved through increasing integration and/or exposure times. Variations due to TVI contrast-agent delivery may be mitigated with blood vessel cannulation in the future.

The current CE $\mu$ CT technique allows for the high-resolution imaging of the mouse IVD *in vivo* at spatial resolutions at tens of microns,<sup>4</sup> and thus can quantify the structural characteristics of the IVD with greater precision and fidelity. In addition, this approach allows for the imaging of multiple spinal sites with a single set up. TVI of loversol was well-tolerated by the mice and demonstrates the feasibility this

technique for longitudinal studies. Previous studies have utilized *in vivo* microCT for longitudinal studies with no adverse events reported due to radiation.<sup>13,14</sup> CE $\mu$ CT will be a valuable strategy for *in vivo* monitoring of IVD injury and degeneration across multiple levels in mouse models.

## ACKNOWLEDGMENTS

The authors acknowledge the support from the Washington University Musculoskeletal Research Center NIH P30 AR057235, NIH UL1 TR002345, NIH T32 DK108742, NIH K01 AR069116, NIH R21 AR069804, and NIH R01 AR074441. Funding sources had no involvement in the study.

## CONFLICT OF INTEREST

All authors state they have no conflicts of interest.

## AUTHOR CONTRIBUTIONS

Remy Walk

1. Performed experiments
2. Analysis and interpretation of the data
3. Drafted manuscript
4. Approved final version of manuscript

Simon Tang

1. Conceived and designed research
2. Analysis and interpretation results of experiments
3. Edited and revised manuscript
4. Approved final version of manuscript

## ORCID

Simon Y. Tang  <https://orcid.org/0000-0002-5570-3921>

## REFERENCES

1. Hoy D, Bain C, Williams G, et al. A systematic review of the global prevalence of low back pain. *Arthritis Rheum.* 2012;64(6):2028-2037.
2. Luoma K, Riihimäki H, Luukkonen R, Raininko R, Viikari-Juntura E, Lamminen A. Low back pain in relation to lumbar disc degeneration. *Spine.* 2000;25(4):487-492.
3. Lotz J. Animal model of intervertebral disc degeneration: lessons learned. *Spine.* 2004;29(23):2742-2750.
4. Kagadis GC, Loudos G, Katsanos K, Langer SG, Nikiforidis GC. *In vivo* small animal imaging: current status and future prospects. *Med Phys.* 2010;37(12):6421-6442.
5. Bouxsein M, Boyd S, Christiansen B, Guldberg R, Jepsen K, Müller R. Guidelines for assessment of bone microstructure in rodents using micro-computed tomography. *J Bone Miner Res.* 2010;25(7):1468-1486.
6. Bhalla S, Lin KH, Tang SY. Postnatal development of the murine notochord remnants quantified by high-resolution contrast-enhanced microCT. *Sci Rep.* 2017;7(1):13361.

7. Newton M, Hartner S, Timmons S, et al. Contrast-enhanced  $\mu$ CT of the intervertebral disc: a comparison of anionic and cationic contrast agents for biochemical and morphological characterization. *J Orthop Res*. 2017;35(5):1067-1075.
8. McClennan BL. Ionic versus nonionic contrast media: safety, tolerance, and rationale for use. *Urol Radiol*. 1989;11(4):200-202.
9. Lin K, Wu Q, Leib D, Tang S. A novel technique for the contrast-enhanced microCT imaging of murine intervertebral discs. *J Mech Behav Biomed Mater*. 2016;63:66-74.
10. Lin K, Tang S. The quantitative structural and compositional analyses of degenerating intervertebral discs using magnetic resonance imaging and contrast-enhanced micro-computed tomography. *Ann Biomed Eng*. 2017;45(11):2626-2634.
11. Dahia C, Mahoney E, Durrani A, Wylie C. Postnatal growth, differentiation, and aging of the mouse intervertebral disc. *Spine*. 2009;34(5):447-455.
12. Holguin N, Aguilar R, Harland R, Bomar B, Silva M. The aging mouse partially models the aging human spine: lumbar and coccygeal disc height, composition, mechanical properties, and Wnt signaling in young and old mice. *J Appl Physiol*. 2014;116(12):1551-1560.
13. Laperre K, Depypere M, van Gestel N, et al. Development of micro-CT protocols for the in vivo follow-up of mouse bone architecture without major radiation side effects. *Bone*. 2011;49(4):613-622.
14. Detombe S, Dunmore-Buyze J, Petrov I, Drangova M. X-ray dose delivered during a longitudinal micro-CT study has no adverse effect on cardiac and pulmonary tissue in C57BL/6 mice. *Acta Radiol*. 2013;54(4):435-441.

**How to cite this article:** Walk RE, Tang SY. In vivo contrast-enhanced microCT for the monitoring of mouse thoracic, lumbar, and coccygeal intervertebral discs. *JOR Spine*. 2019;2:e1058. <https://doi.org/10.1002/jsp2.1058>